

Joannis Papavassiliou

Hadron phenomenology from first-principle QCD studies

Received: date / Accepted: date

Abstract The form of the kernel that controls the dynamics of the Bethe-Salpeter equations is essential for obtaining quantitatively accurate predictions for the observable properties of hadrons. In the present work we briefly review the basic physical concepts and field-theoretic techniques employed in a first-principle derivation of a universal (process-independent) component of this kernel. This “top-down” approach combines nonperturbative ingredients obtained from lattice simulations and Dyson-Schwinger equations, and furnishes a renormalization-group invariant quark-gluon interaction strength, which is in excellent agreement with the corresponding quantity obtained from a systematic “bottom-up” treatment, where bound-state data are fitted within a well-defined truncation scheme.

Keywords Bethe-Salpeter equations · Dyson-Schwinger equations · Gluon propagator · Pinch Technique · Background Field Method

1 Introduction

The spectrum and various physical properties of the mesons are traditionally obtained in the continuum by means of special integral equations, known as Bethe-Salpeter equations (BSEs) [1; 2; 3; 4; 5; 6; 7; 8; 9], whose general form is captured by the diagram in Fig.(1). In this particular eigenvalue equation, Γ denotes the so-called Bethe-Salpeter amplitude, and \mathcal{K} the fully-amputated quark-antiquark scattering kernel. The details of the solutions obtained from BSEs depend crucially on the precise form of \mathcal{K} , and the nonperturbative information included in it. In fact, it is well-known that any self-consistent analysis based on BSEs must be intimately connected with nonperturbative phenomena such as chiral symmetry breaking, and quark and gluon mass generation, which are described by the dynamical equations obeyed by the Green’s functions of the theory, namely the Dyson-Schwinger equations (DSEs) [10; 11]. In this presentation we briefly review recent work that aims at a first-principle derivation of a special component of the BSE kernel [12], and compare the results obtained with phenomenologically successful “bottom-up” versions of the same quantity.

2 Definitions and basic ingredients

In the Landau gauge the gluon propagator is given by

$$i\Delta_{\mu\nu}(p) = -i [g_{\mu\nu} - p_\mu p_\nu / p^2] \Delta(p^2), \quad (1)$$

while the ghost propagator, $D(p^2)$, and its dressing function, $F(p^2)$, are related by $D(p^2) = F(p^2)/p^2$.

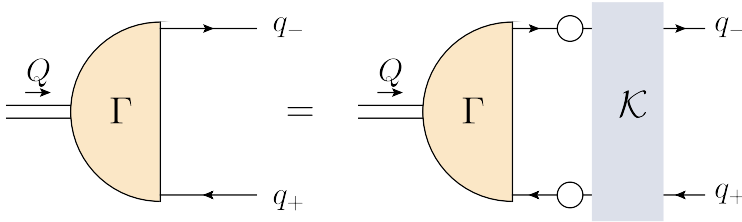


Fig. 1 The meson BSE and the kernel \mathcal{K} .

In addition, consider a special two-point function, denoted by $A_{\mu\nu}(p)$, defined as

$$\begin{aligned} A_{\mu\nu}(p) &= g_{\mu\nu} - ig^2 C_A \int_k H_{\mu\rho}^{(0)} D(k+p) \Delta^{\rho\sigma}(k) H_{\sigma\nu}(-k-p, k, p), \\ &= g_{\mu\nu} [1 + G(p^2)] + \frac{p_\mu p_\nu}{p^2} L(p^2); \end{aligned} \quad (2)$$

where C_A is the Casimir eigenvalue of the adjoint representation, and $\int_k \equiv \mu^{2\epsilon} (2\pi)^{-d} \int d^d k$, with $d = 4 - \epsilon$ the dimension of space-time. The quantity $H_{\mu\nu}$ corresponds to the well-known ghost-gluon kernel that enters in the Slavnov-Taylor identity satisfied by the full three-gluon vertex [13]. In addition, $H_{\mu\nu}$ is related to the full gluon-ghost vertex, Γ_μ , whose tensorial structure is given by

$$-\Gamma_\mu = B_1 p_\mu + B_2 k_\mu, \quad (3)$$

where $B_i = B_i(-k-p, k, p)$, with k representing the momentum of the gluon and p the one of the anti-ghost. Specifically,

$$p^\nu H_{\mu\nu}(-k-p, k, p) = -i\Gamma_\mu(-k-p, k, p). \quad (4)$$

At tree-level, $H_{\mu\nu}^{(0)} = ig_{\mu\nu}$, and $\Gamma_\mu^{(0)} = -p_\mu$.

It turns out that the $1 + G(p^2)$ and $L(p^2)$ defined in Eq. (2) are related to $F(p^2)$ by an exact relation (valid in Landau gauge only) [14]

$$F^{-1}(p^2) = 1 + G(p^2) + L(p^2). \quad (5)$$

3 The universal and renormalization-group invariant part of the BS kernel

Let us consider the kernel appearing in a typical Bethe-Salpeter equation (BSE), shown in Fig.(1), which is contained in the gray box. To make contact with earlier works, we will divide it by a factor of 4π , and will denote it by \mathcal{K} . The kernel \mathcal{K} receives a “universal” (process-independent) contribution, whose origin is the pure gauge sector of the theory; in that sense, this contribution constitutes the common ingredient of any such kernel, regardless of the nature of the particles between which it is embedded.

The systematic diagrammatic identification of the precise pieces that constitute this particular quantity may be carried out following the procedure known in the literature as pinch technique (PT) [15]. In general, the upshot of this construction is the rearrangement of a physical amplitude into sub-amplitudes with very special properties; in particular, one obtains vertices that satisfy QED-like Ward identities and a gluon propagator that captures all the RG logarithms of the theory, see Fig.(2). In fact, it turns out that these latter quantities coincide precisely with the corresponding vertices and gluon propagator defined in the Background Field Method (BFM) [16]. This particular identification persists both perturbatively, to all orders, as well as nonperturbative, at the level of the corresponding DSEs.

In the case of the gluon propagator, the standard $\Delta(p^2)$ defined in Eq. (1), and the scalar cofactor of the PT-BFM gluon propagator, denoted by $\widehat{\Delta}(p^2)$, are related by the exact relation [17]

$$\Delta(p^2) = \widehat{\Delta}(p^2) [1 + G(p^2)]^2. \quad (6)$$

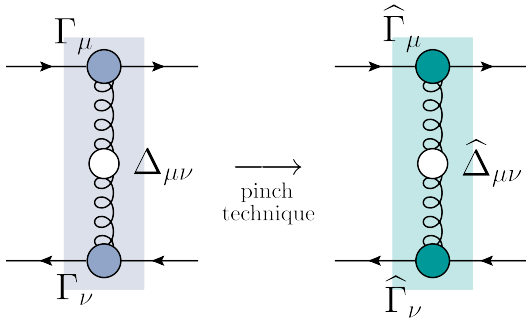


Fig. 2 The one-gluon exchange kernel before and after the pinch-technique rearrangement

At the one-loop level, and keeping only UV logarithms, one has [18]

$$1 + G(p^2) = 1 + \left(\frac{9}{4}\right) \frac{\alpha_s C_A}{12\pi} \ln\left(\frac{p^2}{\mu^2}\right); \quad \Delta^{-1}(p^2) = p^2 \left[1 + \left(\frac{13}{2}\right) \frac{\alpha_s C_A}{12\pi} \ln\left(\frac{p^2}{\mu^2}\right)\right], \quad (7)$$

and thus

$$\widehat{\Delta}^{-1}(p^2) = p^2 \left[1 + b\alpha_s \ln\left(\frac{p^2}{\mu^2}\right)\right], \quad (8)$$

where $b = 11C_A/12\pi$ is the first coefficient of the Yang-Mills β function, as it should [16].

Similarly, the PT-BFM quark-gluon vertex $\widehat{\Gamma}_\mu^a = \frac{\lambda^a}{2} \widehat{\Gamma}_\mu$, which satisfies the QED-like Ward identity

$$q^\mu \widehat{\Gamma}_\mu(q, p_2, -p_1) = S^{-1}(p_1) - S^{-1}(p_2), \quad (9)$$

is related to the conventional Γ_μ by the BQI

$$[1 + G(q^2)]\Gamma_\mu(q, p_2, -p_1) = \widehat{\Gamma}_\mu(q, p_2, -p_1) + S^{-1}(p_1)Q_\mu(q, p_2, -p_1) + \overline{Q}_\mu(-q, p_1, -p_2)S^{-1}(p_2), \quad (10)$$

where $S^{-1}(p)$ is the inverse of the full quark propagator, with $S^{-1}(p) = A(p^2)\not{p} - B(p^2)$, and the quantities Q_μ and \overline{Q}_μ are auxiliary three-point functions containing composite vertices. The important point for what follows is that the last two terms on the rhs of Eq. (10) vanish when the external quarks are on shell; otherwise, they cancel against other (process-dependent) contributions.

To see how these considerations apply to the case at hand, let us express \mathcal{K} in terms of the basic field-theoretic quantities that comprise it, namely (suppressing all spinor indices)

$$\mathcal{K}(p, q_+, -q_-) = \alpha_s \Gamma_\mu(p, q_+, -p - q_+) \left(\frac{\lambda^a}{2}\right) \Delta^{\mu\nu}(p) \left(\frac{\lambda^a}{2}\right) \Gamma_\nu(-p, -q_-, p + q_-), \quad (11)$$

where $\alpha_s = g^2/4\pi$, and g is the gauge coupling.

As a consequence of Eq. (10) and Eq. (6), Eq. (11) may be cast into the equivalent form

$$\mathcal{K}(p, q_+, -q_-) = \alpha_s \widehat{\Gamma}_\mu(p, q_+, -p - q_+) \left(\frac{\lambda^a}{2}\right) \widehat{\Delta}^{\mu\nu}(p) \left(\frac{\lambda^a}{2}\right) \widehat{\Gamma}_\nu(-p, -q_-, p + q_-). \quad (12)$$

In what follows we will focus only on the the part of $\widehat{\Gamma}_\mu$ that is proportional to γ_μ , namely $\widehat{\Gamma}_\mu = \gamma_\mu \widehat{\Gamma}_1 + \dots$, so that the corresponding contribution to the \mathcal{K} of Eq. (12), to be denoted by \mathcal{C} , is given by

$$\mathcal{C}(p, q_+, -q_-) = \underbrace{\alpha_s \widehat{\Delta}(p^2)}_{\text{universal}} \underbrace{[\widehat{\Gamma}_1(p, q_+, -p - q_+) (\gamma_\mu) \left(\frac{\lambda^a}{2}\right) P_{\mu\nu}(p) \left(\frac{\lambda^a}{2}\right) (\gamma_\nu) \widehat{\Gamma}_1(-p, -q_-, p + q_-)]}_{\text{process-dependent}}, \quad (13)$$

Due to the special Ward identities satisfied by the PT-BFM Green's functions [*e.g.*, Eq. (9)], the (dimensionful) universal combination [19]

$$\widehat{d}(p^2) = \alpha_s \widehat{\Delta}(p^2) = \frac{\alpha_s \Delta(p^2)}{[1 + G(p^2)]^2}, \quad (14)$$

introduced in Eq. (13), is also renormalization-group invariant (RGI). Indeed, since $g(\mu^2) = Z_g^{-1}(\mu^2)g_0$ and $\widehat{\Delta}(p^2, \mu^2) = \widehat{Z}_A^{-1}(\mu^2)\widehat{\Delta}_0(p^2)$, where the “0” subscript indicates bare quantities, and the QED-like relation $Z_g = \widehat{Z}_A^{-1/2}$ is valid, we have that

$$\widehat{d}_0(p^2) = \alpha_{s_0}\widehat{\Delta}_0(p^2) = \alpha_s(\mu^2)\widehat{\Delta}(p^2, \mu^2) = \widehat{d}(p^2) \quad (15)$$

maintains the same form before and after renormalization, *i.e.*, it forms a RGI (μ -independent) quantity.

4 Nonperturbative evaluation of $\widehat{d}(p^2)$

In this section we use a combination of lattice results and dynamical equations to determine the nonperturbative form of the fundamental quantity $\widehat{d}(p^2)$ given in Eq. (14). To that end, we will use for $\Delta(p^2)$ the lattice data from [20], whilst for the quantities $1 + G(p^2)$ and $L(p^2)$ we will use the following set of (renormalized) equations

$$\begin{aligned} 1 + G(p^2) &= Z_c + \frac{g^2 C_A}{d-1} \int_k \left[(d-2) + \frac{(k \cdot p)^2}{k^2 p^2} \right] B_1(-k, 0, k) \Delta(k) D(k+p), \\ L(p^2) &= \frac{g^2 C_A}{d-1} \int_k \left[1 - \frac{(k \cdot p)^2}{k^2 p^2} \right] B_1(-k, 0, k) \Delta(k) D(k+p), \end{aligned} \quad (16)$$

where the renormalization constant Z_c is determined from the MOM condition $F(\mu^2) = 1$. The assumptions and approximations employed in the derivation of the above set of equations have been explained in detail elsewhere [14; 19]. In addition, the form factor B_1 that enters in the three equations of (16) has been computed from its own DSE, in the limit of vanishing ghost momentum [21]. Note that even though only $G(p^2)$ enters into the definition of Eq. (14), from Eq. (16) we will determine $G(p^2)$, $L(p^2)$, and $F(p^2)$; this in turn, will allow us to test numerically the validity of Eq. (5), which constitutes a nontrivial check of the entire numerical procedure.

The results of the numerical solution of Eq. (16) are shown in the right panel of Fig. 3. It is clear that the solutions obtained for $1 + G$ and L satisfy the fundamental relation (16) at a high level of accuracy; this provides a non-trivial test for the integration routines used in solving the ghost DSE. Note also that even though $L(p^2)$ vanishes at the origin, it has a non-vanishing support in the region of physical interest (see the top right panel of Fig. 3).

The quantity $\widehat{d}(p^2)$ is RGI, as is evident from the bottom left panel of Fig. 3. There, $\widehat{d}(p^2)$ is shown when evaluated at three different renormalization points: $\mu = 4.3, 3.0$ and 2.5 GeV, for which the corresponding coupling reads $\alpha_s(\mu^2) = 0.22, 0.30$ and 0.36 respectively. As can be seen in the bottom right panel, these values for the strong couplings are in very good agreement with those obtained from detailed calculations of the gauge coupling, α_{MOM} , in the momentum subtraction (MOM) scheme, for values of Λ_{QCD} between 250 and 320 MeV [22].

5 Comparison between “top-down” and “bottom-up” approaches

In order to make contact with the relevant literature on BSEs, we note that the quantity \mathcal{C} appearing in Eq. (13) has been traditionally cast in the form

$$\mathcal{C}(p, q_+, -q_-) = \frac{\mathcal{I}(p^2)}{p^2} \otimes (\text{process} - \text{dependent}), \quad (17)$$

where $\mathcal{I}(p^2)$ is a dimensionless quantity, which may be interpreted as the effective interaction strength of the quark-gluon system. Evidently, in the PT-BFM case one must extract an analogous quantity from the $\widehat{d}(p^2)$ of Eq. (14) through multiplication by p^2 , namely

$$\mathcal{I}(p^2) = p^2 \widehat{d}(p^2). \quad (18)$$

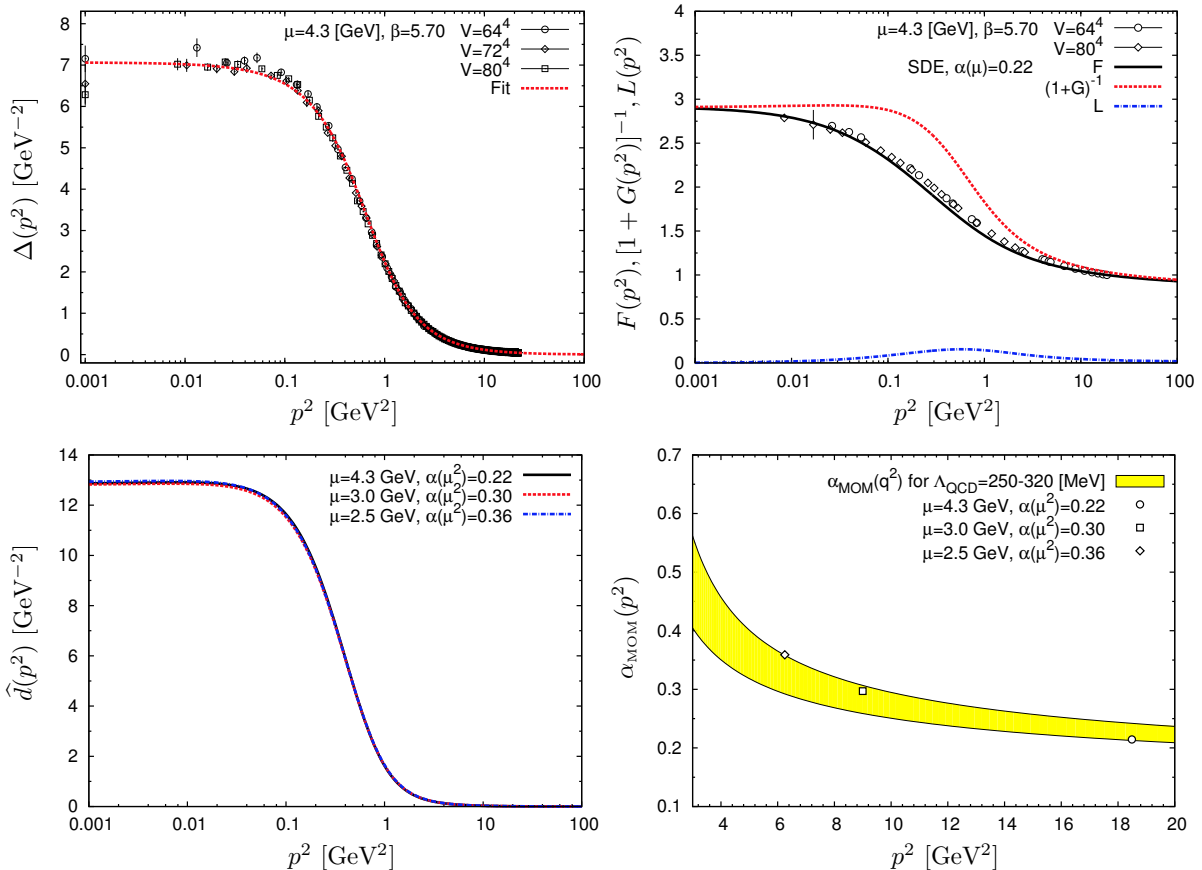


Fig. 3 The Landau gauge gluon propagator (top left panel) used for the numerical evaluation of the DSEs in (16) (top right panel) for the case $\mu = 4.3$ GeV (lattice data are from of [20]). The RGI quantity $\hat{d}(p^2)$ evaluated at $\mu = 4.3, 3.0$ and 2.5 GeV (bottom left panel). The resulting curves are then rescaled by $\alpha_s(\mu^2) = 0.22, 0.30$ and 0.36 , respectively, in compliance with values obtained for α_{MOM} when Λ_{QCD} varies between 250 and 320 MeV (yellow band on the bottom right panel) [22].

At this point, the $\mathcal{I}(p^2)$ obtained from Eq. (18) can be compared with the corresponding quantities defined in the bottom-up framework. As reviewed elsewhere (see, *e.g.*, [23]), successful explanations and predictions of numerous hadron observables can be obtained by choosing

$$\mathcal{I}(p^2) = p^2 \mathcal{G}(p^2); \quad \mathcal{G}(p^2) = \frac{8\pi^2}{\omega^4} D e^{-p^2/\omega^2} + \frac{8\pi^2 \gamma_m (1 - e^{-p^2/4m_t^2})}{k^2 \ln[\tau + (1 + p^2/\Lambda_{\text{QCD}}^2)^2]}, \quad (19)$$

where $\gamma_m = 12/(33 - 2N_f)$ [typically, $N_f = 4$], $\Lambda_{\text{QCD}} = 0.57$ GeV (in the MOM scheme); $\tau = e^2 - 1$, $m_t = 0.5$ GeV. Note that D and ω are not independent, but must be related by $D\omega = (\zeta_G)^3 = \text{const}$ and $\omega \in [0.4, 0.6]$ GeV; then, one can reproduce a large body of observable properties of ground-state vector- and isospin-nonzero pseudoscalar mesons, as well as various properties of the nucleon and Δ resonance [25]. The parameter ζ_G is fixed by requiring that the correct value of the pion decay constant f_π is reproduced; its precise value depends on the vertex Ansatz employed.

In the case of the rainbow-ladder (RL) truncation [24], corresponding to $\Gamma^\nu \sim \gamma_\nu$, one has $\zeta_{\text{RL}} = 0.87$ GeV. Instead, the improved truncation scheme of [25], which incorporates dynamical chiral symmetry breaking (DB) effects by using a more sophisticated representation for Γ^ν , gives $\zeta_{\text{DB}} = 0.55$ GeV.

The results of the top-down approach of [12] (denoted by DSE), and the two bottom-up approaches (RL and DB) summarized above, are shown in Fig. (4). It is clear that while the RL interaction strength is far larger than that of the DSE, the comparison between the DB and DSE results is very favorable. Evidently, the DB approach captures corrections that are not included in the RL, and is therefore much closer to the DSE result (see also [26]).

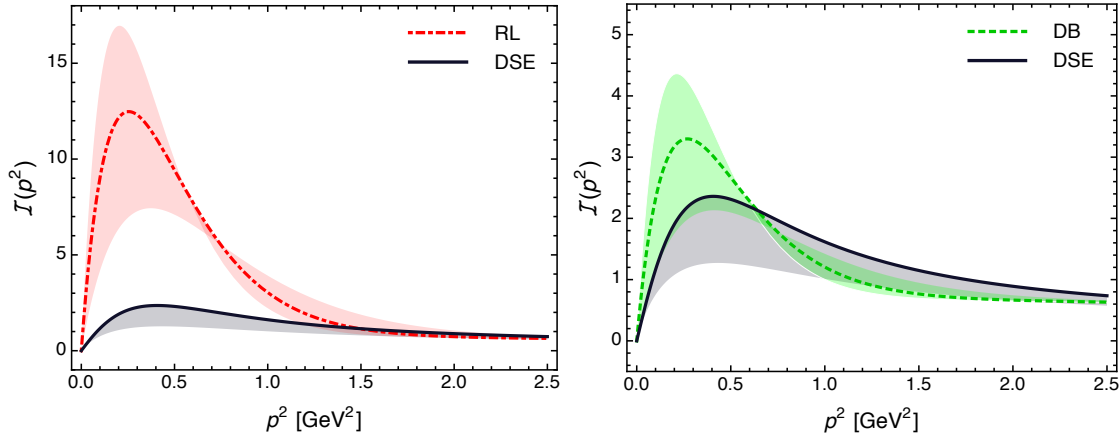


Fig. 4 Comparison of the interaction strength \mathcal{I} evaluated in the RL, IRL and DSE schemes. The shaded areas represent phenomenologically acceptable ranges.

6 Conclusions

In this work we have reviewed recent developments towards a first-principle derivation of the BSE kernel from the dynamical equations obtained from the QCD Lagrangian. This particular effort, in turn, bridges to a large extent the gap between nonperturbative continuum QCD studies and bound-state phenomenology.

Acknowledgements This research is supported by the Spanish MEYC under grants FPA2011-23596, FPA2014-53631-C2-1-P, and SEV-2014-0398, and the Generalitat Valenciana under grant PrometeoII/2014/066. I would like to thank the organizers for their kind invitation and their warm hospitality during the workshop.

References

1. P. Jain and H. J. Munczek, *Phys. Rev. D* **48**, 5403 (1993).
2. H. J. Munczek, *Phys. Rev. D* **52**, 4736 (1995).
3. A. Bender, C. D. Roberts and L. Von Smekal, *Phys. Lett. B* **380**, 7 (1996).
4. P. Maris, C. D. Roberts and P. C. Tandy, *Phys. Lett. B* **420**, 267 (1998).
5. A. Bender, W. Detmold, C. D. Roberts and A. W. Thomas, *Phys. Rev. C* **65**, 065203 (2002).
6. L. Chang and C. D. Roberts, *Phys. Rev. Lett.* **103**, 081601 (2009).
7. C. S. Fischer and R. Williams, *Phys. Rev. Lett.* **103**, 122001 (2009).
8. G. Eichmann, arXiv:0909.0703 [hep-ph].
9. G. Eichmann, I. C. Cloet, R. Alkofer, A. Krassnigg and C. D. Roberts, *Phys. Rev. C* **79**, 012202 (2009).
10. C. D. Roberts and A. G. Williams, *Prog. Part. Nucl. Phys.* **33**, 477 (1994).
11. P. Maris and C. D. Roberts, *Int. J. Mod. Phys. E* **12**, 297 (2003).
12. D. Binosi, L. Chang, J. Papavassiliou and C. D. Roberts, *Phys. Lett. B* **742**, 183 (2015).
13. J. S. Ball and T. W. Chiu, *Phys. Rev. D* **22**, 2550 (1980); [*Phys. Rev. D* **23**, 3085 (1981)].
14. A. C. Aguilar, D. Binosi and J. Papavassiliou, *JHEP* **0911**, 066 (2009).
15. See, for example, D. Binosi and J. Papavassiliou, *Phys. Rept.* **479**, 1 (2009).
16. L. F. Abbott, *Nucl. Phys. B* **185**, 189 (1981).
17. D. Binosi and J. Papavassiliou, *Phys. Rev. D* **66**, 025024 (2002).
18. A. C. Aguilar, D. Binosi and J. Papavassiliou, *Phys. Rev. D* **78**, 025010 (2008).
19. A. C. Aguilar, D. Binosi, J. Papavassiliou and J. Rodriguez-Quintero, *Phys. Rev. D* **80**, 085018 (2009).
20. I. L. Bogolubsky, E. M. Ilgenfritz, M. Muller-Preussker and A. Sternbeck, *Phys. Lett. B* **676**, 69 (2009).
21. A. C. Aguilar, D. Ibanez and J. Papavassiliou, *Phys. Rev. D* **87**, no. 11, 114020 (2013).
22. P. Boucaud, F. De Soto, J. P. Leroy, A. Le Yaouanc, J. Micheli, O. Pene and J. Rodriguez-Quintero, *Phys. Rev. D* **79**, 014508 (2009).
23. I. C. Cloet and C. D. Roberts, *Prog. Part. Nucl. Phys.* **77**, 1 (2014).
24. P. Maris and P. C. Tandy, *Phys. Rev. C* **60**, 055214 (1999).
25. S. x. Qin, L. Chang, Y. x. Liu, C. D. Roberts and D. J. Wilson, *Phys. Rev. C* **84**, 042202 (2011).
26. D. Binosi, L. Chang, J. Papavassiliou, S. X. Qin and C. D. Roberts, arXiv:1601.05441 [nucl-th].